Article

Site-Specific Seed Yield Prediction of Red Fescue (*Festuca rubra* L.) Based on Drone Imaging and Local Regression Models

Christian Andreasen [1,2,*,†], Jesper Rasmussen [1,†] and Zahra Bitarafan [2]

1 Department of Plant and Environmental Sciences, University of Copenhagen, Højbakkegaard Allé 13, 2630 Taastrup, Denmark
2 Division of Biotechnology and Plant Health, Norwegian Institute of Bioeconomy Research (NIBIO), Høgskoleveien 7, 1433 Ås, Norway
* Correspondence: can@plen.ku.dk; Tel.: +45-35-333-453
† These authors contributed equally to this work.

Abstract: Yield maps give farmers information about growth conditions and can be a tool for site-specific crop management. Combine harvesters may provide farmers with detailed yield maps if there is a constant flow of a certain amount of biomass through the yield sensor. This is unachievable for grass seeds because the weight of the intake is generally too small to record the variation. Therefore, there is a need to find another way to make grass seed yield maps. We studied seed yield variation in two red fescue (*Festuca rubra*) fields with variation in management and soil fertility, respectively. We estimated five vegetation indices (VI) based on RGB images taken from a drone to describe yield variation, and trained prediction models based on relatively few harvested plots. Only results from the VI showing the strongest correlation between the index and the yield are presented (Normalized Excess Green Index (ExG) and Normalized Green/Red Difference Index (NGRDI)). The study indicates that it is possible to predict the yield variation in a grass field based on relatively few harvested plots, provided the plots represent contrasting yield levels. The prediction errors in yield (RMSE) ranged from 171 kg ha^{-1} to 231 kg ha^{-1}, with no clear influence of the size of the training data set. Using random selection of plots instead of selecting plots representing contrasting yield levels resulted in slightly better predictions when evaluated on an average of ten random selections. However, using random selection of plots came with a risk of poor predictions due to the occasional lack of correlation between yield and VI. The exact timing of unmanned aerial vehicles (UAVs) image capture showed to be unimportant in the weeks before harvest.

Keywords: aerial images; crop color; creeping red fescue; drone imaging; local regression models; slender creeping red fescue

1. Introduction

Yield mapping is an essential component of precision agriculture [1]. Combine harvesters equipped with yield monitors consisting of yield sensors and global navigation satellite systems (GNSS) were crucial elements in the development of precision agriculture because they were one of the first means to characterize the within-field variability in crop yield [1–3]. Yield monitors have been available on the market since the early 1990s, and there is comprehensive research on yield monitoring and yield variability within fields [4,5].

The global level of adoption of yield monitoring and yield maps is relatively unknown. Most existing studies focus on North America, which has the greatest adoption level [6,7]. Schimmelpfennig [7] reported that yield monitors were used on roughly 70% of the United States corn and soybean acres in 2010–2012. European studies indicate lower levels of adoption [8], and there is evidence that most yield monitors are used to visualize the real-time yield during harvest and not as data providers for yield maps [7,8]. Lachia et al. [8] reported that the use of yield maps is too complex for the majority of farmers.

Despite the apparent challenges of using yield monitors to produce yield maps as a basis for decision-making, the scientific community's interest in yield monitoring has decreased during the last decades [9]. Research seems to have lost its attractiveness in favor of newer topics such as remote sensing [10] and the use of unmanned aerial vehicles (UAVs) [11].

Crop yield predictions are based on either data-driven or process-based models. In data-driven models, empirical models are based on observed data, such as vegetation indices (VI) derived from spectral sensing and corresponding crop yields [12]. Such models are considered black-box models since they do not explain the mechanism that drives the yield. Nevertheless, they are evaluated to be the most practical models for yield predictions with few inputs [13] and are useful for precision agricultural contexts. Detailed information on crop growth and phenology is required to achieve information about the mechanisms behind the yield. Process-based models are helpful in regional yield forecasting systems [14] but far too data demanding in precision agricultural contexts.

Regarding grass seed production, knowledge about yield variability within fields is particularly sparse. To the authors' knowledge, only one study in perennial ryegrass (*Lolium perenne* L.) has been published, concluding that the yield estimates of yield monitors on combine harvesters vary substantially from previous or subsequent observations, even over an apparently uniform ryegrass field [15]. The main reasons are that the amount of seed biomass or seed volume is significantly less than for cereals, maize, and soybean and that the biomass of stems, leaves and chaff (material other than grain) is relatively greater. Therefore, it is not possible to achieve reliable yield maps based on data from yield monitors mounted on combine harvesters.

The increasing use of UAVs opens new possibilities for remote sensing of crops and providing yield estimates [16]. A simple approach in yield estimation based on UAV imagery is to establish relationships between VI and crop yield [17]. VI are computed using several spectral bands sensitive to plant biomass and vigor, and there are two major groups of VI. One group includes spectral bands in the invisible spectrum, and another includes spectral bands exclusively in the visible spectrum. The first group requires multispectral cameras for image acquisition, and the second group can be acquired with RGB cameras. Both types of VI may be suitable for yield estimations [18] because they reflect the vigor, LAI, and other physical characteristics of the crop [19].

Suppose it is possible to establish linear or non-linear relationships between VI and crop yield, then regression models can be used to predict yield. In a previous study, Jensen et al. [20] investigated different selection strategies for training regression models to predict the density of annual grass weeds in cereals based on VI derived from UAV color images. The study showed that training based on selection from extreme values in the field provided better prediction accuracy than random selection. Furthermore, the study showed that simple linear prediction models offered a valuable alternative to a more complex random forest machine-learning algorithm [20].

The color, and thereby the spectral signature, of red fescue crops depends on several factors such as the degree of lodging, the variety, the fertilizer, soil conditions, and drought [21]. The seed yield is also affected by the time that lodging and fertilization take place [21]. Therefore, it is extremely difficult to develop generalized models describing the relation between spectral characteristics and the yield variation in a specific field. In general, research in yield predictive models should focus on generalized models to be applied elsewhere and across various temporal scales. However, this study motions for the opposite because generalized models related to grass seed production are out of immediate reach. In consequence, this study applies a simplistic field specific approach, making it possible to achieve information about yield variation in grass seed crops.

This study aims to evaluate to what degree it is possible to predict yield in red fescue (*Festuca rubra* L.) based on regression models using crop yield from plots with extreme yields and VI from UAV RGB imagery in specific fields. It is hypothesized that (a) an increasing number of plots used for training increases the predictive power, (b) training

based on plots with extreme VI values increase the predictive power compared to random plot selection, and (c) the exact timing of drone imagery is of minor importance if crop heterogeneity is visible for a longer period.

2. Materials and Methods

2.1. Experimental Approach

The underlying idea was to establish field-specific prediction models based on yield sampling and drone-derived VI. The experimental fields must have recognizable yield variations because we want to test whether a regression model can be developed to estimate the yield based on sampling of extreme yields. Hence, the first step is to define areas in the field with minimum and maximum yields. The following steps are to acquire UAV images of the whole field and to sample yields from the areas with extreme yields. After that, a vegetation index derived from the UAV imagery that correlates with the sampled crop yields must be identified. Finally, crop yield for the entire field is predicted based on a field-specific regression model that connects yield and a suitable VI. In this study, yield sampling was carried out with an experimental combine harvester and VI were based on RGB images derived from a UAV.

2.2. Field Experiments

This study was carried out in two fields with red fescue (*Festuca rubra* L.). The first field consisted of 96 plots, which were established to investigate the impacts of a plant growth regulator (PGR) on lodging and yield. All plots were harvested in 2018, and results have been reported elsewhere [21]. The second field was a commercial field with heterogeneous growth believed to be a result of variable soil fertility. Differences in growth could be recognized throughout the growing season as differences in crop color and vigor. In this field, 20 plots were harvested in 2020 and used for training and prediction. In both years, the plot size was 1.5×12 m. In 2018, 10, 20, and 48 plots were used to train a regression model and, in 2020, 6 and 10 plots were used for training. Images were collected on clear and sunny days with few cumulus clouds that did not shade the sun during image acquisition. In both fields, herbicides and fungicides successfully controlled weeds and diseases.

2.2.1. Field Experiment Harvested in 2018

The field experiment was established in 2015 at the research station of the University of Copenhagen, Taastrup (55°40′8.16″ N; 12°18′18.82″ E), Denmark, in a field with clay loam soil (Figure 1). Red fescue (cv. Maxima) was under-sown in spring barley (cv. Odyssey) on 15 April 2015, and the experimental treatments consisted of four seeding rates (2, 4, 6, and 8 kg ha^{-1}) and four PGR application rates of Moddus M (250 g l^{-1} trinexapac-ethyl, Syngenta Nordic A/S). Experimental details and results are given in Bitarafan et al. [21]. PGR affected yield, whereas the seeding rates had no impact. The grass seed plots were harvested for three consecutive years (8 July in 2016; 17 July in 2017; 3 July in 2018), and seeds were air-dried and cleaned after harvest. In this study, only yields from 2018 are presented because UAV images were not acquired in the previous years.

2.2.2. Field Experiment Harvested in 2020

A 1.6 ha red fescue (cv. Maxima) field with clayey soil was established in 2018 at the research station of the University of Copenhagen in Taastrup (55°40′8.16″ N; 12°18′18.82″ E), Denmark. Red fescue was undersown in winter wheat (cv. KWS Lilli) the day after winter wheat establishment on 20 September 2018. Fertilizer and pesticide applications were used according to commercial farming practice to achieve the most profitable yield. Just before harvest in 2020, 20 plots distributed all over the fields were marked, representing large yield variation based on visual inspection of the field (Figure 2).

Figure 1. UAV image of the experimental plots from 2018, University of Copenhagen, Taastrup (55°40′8.16″ N; 12°18′18.82″ E).

Figure 2. UAV image of the field and plots from 24 June 2020. The red markings show the plots where seed yields were harvested, University of Copenhagen in Taastrup (55°40′8.16″ N; 12°18′18.82″ E).

The field was harvested on 14 July 2020 except for the marked plots, which were harvested on 1 August with a plot combine harvester. From each plot, the grass seeds were air-dried, and after cleaning, seed samples were weighed, and the weight converted to seed yield ha^{-1}.

2.3. Drone Images

UAV images were captured with a Phantom 4 (DJI, Shenzhen, China) quadrotor equipped with a built-in GNSS and an integrated RGB camera before harvest on 27 June 2018 (Figure 1) and on 17 July 2020 (Figure 2). In 2020, UAV images were also captured before plots were marked on 3 March, 13 May, 26 May, and 24 June to investigate the importance of timing. On these dates, plots were identified after alignment with the 17 July orthomosaic where plots were visible.

Images were captured at noon +/− 2 h. Ground control points (GCPs) were used for geometric correction of orthomosaics. In each field, the position of ten visible markers were measured using Trimble R10 GNSS with TSC3 controller (Trimble, Sunnyvale, CA, USA). The positioning system receives correction signals from GPSnet.dk (Geoteam, Ballerup, Denmark), a Danish network of ground-based reference stations based on Trimble's VRS technology (Trimble, Sunnyvale, CA, USA). This provided an accuracy of 0.02 m after post-processing.

The camera was a Sony 12.4 megapixel with a $1/2.3'$ CMOS sensor (4000×3000 pixels). The flight altitude was 40 m according to onboard barometer measurements, and the ground sampling distance (GSD) was 1.7 cm pixel^{-1}. However, the precise flight altitude is considered of minor importance [19]. Images were captured under stable light conditions. The frontal overlap of images with respect to the flight direction was 80%, and the lateral overlap was 70%. Average flight duration was 2.5 min ha^{-1}. Orthomosaics were generated in Pix4DMapper version 5.6.1, and plots were cropped from the orthomosaics with the open-source GIS software QGIS (https://www.qgis.org/en/site/ (accessed on 17 January 2023)) version QGIS 2.18.1 Long Term Release (LTR), QGIS Development Team QGIS Geographic Information System. Open Source Geospatial Foundation Project (http://qgis.org (accessed on 17 January 2023). The average size of orthomosaics was 120 MB per hectare. The spatial accuracy of created orthomosaics was less than 5 cm.

The mean values of the raw digital numbers of the red (R), green (G), and blue (B) bands for each plot were calculated in QGIS. There were no color calibrations.

2.4. Selection of Plots

The selection of plots for the training of the field-specific regression models was based on a combination of color variation in UAV photos and visual assessments of the crop yield on the ground to identify a wide range of crop yields. In 2018, the color variation in UAV photos constituted the selection criteria because there was a large variability in lodging. Lodging and color have previously been shown to correlate [21], and it was assumed that yield and lodging were correlated based on visual inspections in the field. In 2020, selection of plots was based on visual yield inspections in the field. In 2018, 10, 20, and 48 plots were selected for training, and in 2020, 6 and 10 plots were selected for training to investigate the importance of an increasing number of plots used for training. Two criteria were used for the selection of training plots: (a) extreme VI values (the independent regression variable) and (b) random selection. A random selection was conducted to test the hypothesis that plots with extreme values of VI would increase the predictive power compared to a random selection of plots. The selection of random plots was repeated ten times for each number of training plots.

2.5. Vegetation Indices

We considered five vegetation indices (VI) based on the R (red), G (green), and B (blue) bands for the prediction models:

$$\text{Normalized Excess Green Index (ExG)} = (2 \times G - R - B)/(R + B + G) \tag{1}$$

$$\text{Excess Green index (ExG)—Excess Red index (ExR)} = 2 \times G - R - B - 1.4 \times R + G \tag{2}$$

$$\text{Normalized difference index (NGRDI)} = (G - R)/(G + R) \tag{3}$$

$$\text{RB ratio} = R/B \tag{4}$$

$$\text{Red index} = 2 \times \text{R} - \text{G} - \text{B} \tag{5}$$

In addition to the five indices, the blue band (B) and the sum of R, G, and B were used as well. Mean values for each plot of the digital numbers (0–255) for R, G, and B were used in the calculations. Only results from the VI showing the strongest correlation between the index and the yield are presented (ExG [22] and NGRDI [23]).

2.6. Statistical Analyses

We used an increasing number of plots to train the field-specific linear regression models based on the two indices (ExG and NGRDI) to describe the relationship between the VI and the crop yield. The index obtaining the highest correlation was used to predict the yield, and the root mean square error (RMSE) was calculated to evaluate the predictive performance. RMSE reflects the average distance between the predicted yield and the actual yield and was calculated in absolute (kg ha^{-1}) and relative terms (RMSE%). Predictions and RMSE were calculated for both training data sets and validated on the remaining part of the data sets. The minimum achievable RMSE was calculated based on regression analysis on the validation data sets. It reflected how well the validation data could be described by linear regression. Statistical analyses were conducted using the SAS® version 9.4 software (SAS Institute Inc., Cary, NC, USA). PROC CORR was used for correlation analysis and PROC GLM was used for parameter estimation and F-tests to evaluate the effect of training data set size on regression parameters. PROC GLM was used to calculate prediction intervals for any specific VI value. There is 95% probability that the real yield is within the calculated prediction interval for a specific VI value. The random selection of plots for training was carried out by using the UNIFORM function in SAS. The random selection was repeated ten times for each number of plots used for training.

3. Results

In 2018, the average yield was 1548 kg ha^{-1} with a standard deviation of 209 kg, and in 2020, the average yield was 1160 kg ha^{-1} with a standard deviation of 260 kg. Hence, the absolute and relative crop yield variation was larger in 2020.

ExG correlated slightly better with yield than NGRDI in 2018, whereas it was the opposite in 2020. When half of the plots were used for training (48 plots in 2018 and 10 plots in 2020), the correlation coefficients were 0.71 for ExG (Table 1) and 0.69 for NGRDI in 2018. In 2020, the correlation coefficients were 0.77 for ExG and 0.80 for NGRDI (Table 1).
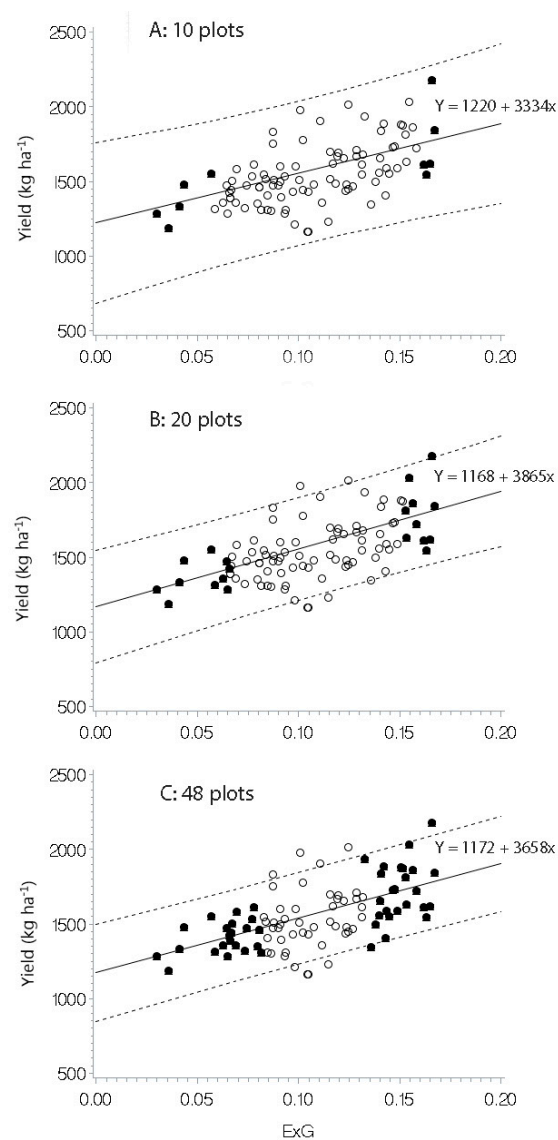
Table 1. Correlation between vegetation indices (VI) and yield in training data sets and yield predictions for the remaining part of data sets. Selection of data from extremes.

Year VI	Training				Yield Prediction for Remaining Data Set	
	Number of Plots Used for Training	Correlation Coefficient [1]	RMSE [2] (kg ha^{-1})	RMSE (%)	RMSE (kg ha^{-1})	RMSE (%)
2018 ExG	10	0.76 *	178	11.5	171	11.1
	20	0.81 ***	193	12.5	184	12.5
	48	0.71 ***	145	9.4	192	12.4
2020 NGRDI	6	0.84 *	118	10.2	231	20.0
	10	0.80 **	182	15.7	222	19.1

[1] * denotes $p < 0.05$; ** denotes $p < 0.01$; *** denotes $p < 0.001$; [2] RMSE = The root mean square error for the model.

Results did not support the hypothesis that the yield prediction accuracy was increased by using an increasing number of training plots. This was found when training was carried out on systematically selected plots (extreme values) (Table 1) and randomly selected plots (Table 2). In both years, parameters in the regression models based on extreme values were not statistically affected by the size of training data sets according to F-tests, which means that RMSE for predictions were more or less unaffected by the size of the training

data sets (Figures 3 and 4). However, the RMSE slightly increased in 2018 with the larger training set (Table 1). A large training set means that the regression model was tested on medium yields only. The opposite trend appeared in 2020, where the largest RMSE were for the extreme yields (Table 1). The minimum achievable RMSE in 2018 was 167 kg ha^{-1}, 172 kg ha^{-1}, and 190 kg ha^{-1} when 10, 20, and 48 plots were used for training. In 2020, the minimum achievable RMSE was 137 kg ha^{-1} and 127 kg ha^{-1} when 6 and 10 plots were used for training.
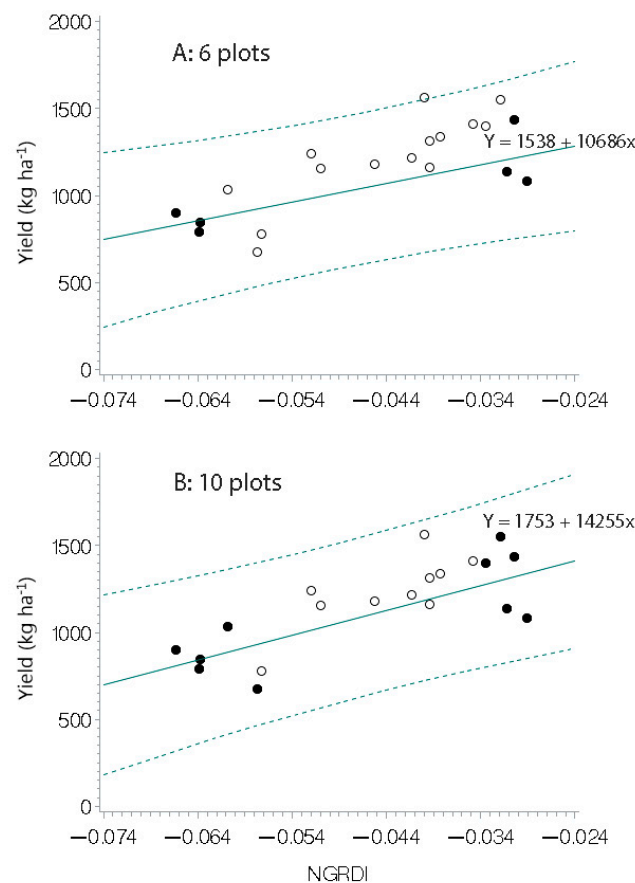

Figure 3. Linear regression models (solid line) with prediction intervals (dotted lines) for specific VI values based on an increasing number of plots in 2018. The model in A is based on 10 plots, B is based on 20 plots and C is based on 24 plots. Plots used in regression analyzes are denoted with dots and validation plots are denoted with open circles. The selection of training data was based on extreme ExG values.

Table 2. Correlation between vegetation indices (VI) and yield in training data sets and yield predictions for the remaining part of the data sets. Random selection of data based on 10 random selections for each number of plots.

Year VI		Training		Yield Prediction for Remaining Data Set (Average of 10 Runs)	
	Number of Plots Used for Training	Average Correlation Coefficient	Range of Correlation Coefficients [1]	RMSE [2] (kg ha^{-1})	RMSE (%)
2018 ExG	10	0.67	0.41 *–0.85 **	171	11.1
	20	0.61	0.48 *–0.75 ***	173	11.1
	48	0.59	0.46 *–0.70 ***	191	12.3
2020 NGRDI	6	0.78	0.03^{NS}–0.99 ***	146	12.6
	10	0.83	0.67 *–0.96 ***	130	11.2

[1] NS denotes $p > 0.05$; * denotes $p < 0.05$; ** denotes $p < 0.01$; *** denotes $p < 0.001$; [2] RMSE = The root mean square error for the model.

Figure 4. Linear regression models (solid line) with prediction intervals (dotted lines) for specific VI values based on an increasing number of plots in 2020. The model in A is based on 6 plots and B is based on 10 plots. Plots used in the regression analyzes are denoted with dots and validation plots are denoted with open circles. The selection of training data was based on extreme NGRDI values.

In 2018, the selection criteria of test plots (extreme or random) were unimportant, if the benchmark for the randomly selected plots was average RMSE (Tables 1 and 2). However, as indicated by the range of training correlation coefficients (Table 2), there is a risk of poor yield prediction due to low correlations between yield and VI when training data is randomly selected. In 2020, the average prediction power based on models with randomly selected training data performed better than models training on extreme values (Table 2).

The timing of the UAV image capture was unimportant in 2020 in weeks before harvest. The correlation between NGRDI and yield was 0.49 ($p < 0.05$), 0.68 ($p < 0.001$), 0.76

($p < 0.001$), 0.79 ($p < 0.001$), and 0.77 ($p < 0.001$) on 3 March, 13 May, 24 May, 24 June, and 17 July, respectively.

4. Discussion

Trained local (field-specific) regression models based on UAV imagery showed to be a promising tool for generating yield maps. The yield predictions errors (RMSE) were in the range of 171 kg ha^{-1} to 222 kg ha^{-1} when training data sets consisted of 10 plots and training was based on extreme VI values (Table 1). Different VI gave the best predictive power in different years (Table 1). This was expected because yield variations may have different visual representations in different years and fields. For example, lodging may be negatively correlated with yield if it occurs early in the growing season before pollination [21]. In 2018, lodging showed clearly visible effects in UAV images (Figure 1), whereas it played a minor role in 2020 (Figure 2). Lodging may also be positively correlated with yield if it occurs late in the growing season because of heavy fertile tillers. In 2020, soil fertility had an impact on the greenness of the crop throughout the growing season, which was expressed in NGRDI.

In 2020, the exact timing of UAV image capture was shown to be unimportant in the weeks before harvest because yield variation was related to general growth conditions in the field. The underlying mechanism was possibly caused by soil fertility because crop growth variation was visible throughout the growing season. Therefore, it was possible to establish a significant correlation ($p < 0.05$) between NGRDI and yield in the early spring (3 March 2020). UAV imaging throughout the growing season can be helpful to obtain an understanding of why and when lodging has taken place. It may indicate whether lodging is caused by high yields or heavy rainfall, or insufficient application of plant growth regulators before the pollination had taken place, resulting in a potential low yield, or perhaps a mixture resulting in site-specific variations.

The basic idea of this study was to train regression models based on extreme VI values, but the results showed that random selection of data might provide similar or even better results. With random selection, however, there is a risk of poor correlation between VI and yield (Table 2), leading to poor predictions (Table 2). In 2018, the predictions were close to optimum for the suggested prediction method based on extreme values, because RMSE approached the minimum achievable RMSE values. In 2020, selection of plots covering the whole range of VI would probably have been better because RMSE values were significantly greater than the minimum achievable RMSE and because random selection of plots for training showed lower RMSE. Therefore, the results indicate that it is not necessary only to use extreme values.

The study showed that there is no general relationship between canopy color and yield between fields, and consequently, there is no general relationship between a specific VI and yield. This calls for local models based on field-specific training. Yield predictions based on remote sensing have been investigated thoroughly [24]. Still, the experimental approach in our study differs from the majority of the previous studies [25–28], which investigated advanced machine learning algorithms to make out-of-sample predictions (global models). This means that field-specific training can be avoided in opposite to the approach presented in our study. This may appear as an important advantage, but from an applied perspective, local models may have one significant advantage compared to global automated algorithms: robustness.

Furthermore, global models do not currently exist and there are no indications that such models will be developed in the foreseeable future. As a result, the only practical way to generate yield maps using prediction models is currently by implementing models that are trained specifically for each field. The training aspect is not necessarily a decisive barrier for implementation. Rasmussen et al. [29] approach for detecting and mapping thistles (*Cirsium arvense* L.) based on a local trained model was successfully integrated into Danish farmers' CropManger IT-platform (https://cropmanager.dk/ (accessed on 17 January 2023)). Like for thistle detection, there will be preconditions that need to be met for reliable yield predictions. Clear correlation between yield and colors in drone

images must exist. This will not be the case if the yield variability within a field might be a result of different causes giving different spectral signatures. If lodging is determining yield in some part of the field as in the 2018 experiment, and general growth conditions are determining yield in other parts of the field as in the 2020 experiment, the presented regression approach may fail. Therefore, the regression approach has its limitations, but future studies or practical experiences will have to show whether these limitations are crucial. The limitations of the regression approach depend largely on the nature of the variability, which occurs in grass seed fields. The nature and the extent of this variability has not been studied yet.

In a practical perspective, the cost of training local models must be considered. The main challenges are to obtain reliable yield data from contrasting yield environments and to match plots on ground and in UAV mosaics and to identify a VI that correlates with yield. UAV image acquisition is a prerequisite for both global and local models. It is hardly likely that farmers themselves will undertake all work tasks, which indicates that yield maps based on UAV imagery most likely must be produced by service providers or research institutions. Whether farmers are willing to pay for yield maps is beyond the scope of this article, but it could be argued that yield maps in grass seed crops at present is primary relevant for experimental purposes.

5. Conclusions

The trained local (field-specific) regression models, based on seed yields from a limited number of plots with extreme yields and UAV imagery, predicted the site-specific yields within fields well. The method seems to be a promising tool for making detailed yield maps of red fescue fields. The yield prediction errors (RMSE) were in the range of 171 kg ha^{-1} to 231 kg ha^{-1}. We could not confirm the hypothesis that an increasing number of plots used for training improves the predictive power. Random selection of plots for training gave similar or better predictions on average but with the risks of poor prediction. The timing of the UAV image capture in 2020 was not important in the weeks before harvest because there was no lodging before harvest and crop growth variations were visible throughout the growing season.

Site-specific management of grass fields is challenging, as seed biomass and volume are significantly less than for cereals and difficult to quantify with ordinary yield sensors. Our experiments specify a new method of making reliable yield maps in grass seed production. We suggest that our method should be tested in other grass fields and under other growing conditions to verify the method.

Author Contributions: C.A. was responsible for funding acquisition and the design of the experiments. Z.B. and C.A. were responsible for establishing the experiments. J.R. captured, analyzed UAV images, processed the images, and did the statistical analyses. C.A. wrote the first draft of the article, and all authors reviewed, edited, and accepted the final manuscript. C.A. and J.R. contributed equally to the project and the publication. All authors have read and agreed to the published version of the manuscript.

Conflicts of Interest: The authors declare no conflict of interest. The funders had no role in the design of the study, in the collection, analyses, or interpretation of data, in the writing of the manuscript, or in the decision to publish the results.

References

1. Fulton, J.; Hawkins, E.; Taylor, R.; Franzen, A. Yield Monitoring and Mapping. In *Precision Agriculture Basic*; Kent Shannon, D., David, E.C., Newell, R.K., Eds.; American Society of Agronomy, Crop Science Society of America, Soil Science Society of America: Madison, WI, USA, 2018; p. 5585. [CrossRef]
2. Fountas, S.; Pedersen, S.M.; Blackmore, S. ICT in precision agriculture—Diffusion of technology. In *Ebook: ICT in Agriculture. Perspectives of Technological Innovation*; Gelb, E., Offer, A., Eds.; The Robert H. Smith Faculty of Agriculture, Food and Environment: Rehovot, Israel, 2005; Available online: https://economics.agri.huji.ac.il/sites/default/files/agri_economics/files/gelb-pedersen-5.pdf (accessed on 17 January 2023).
3. Ping, J.L.; Dobermann, A. Processing of yield map data. *Precis. Agric.* **2005**, *6*, 193–212. [CrossRef]
4. Chung, S.O.; Choi, M.C.; Lee, K.H.; Kim, Y.J.; Hong, S.J.; Li, M. Sensing technologies for grain crop yield monitoring systems: A review. *J. Biosystems Engineer.* **2016**, *41*, 408–417. [CrossRef]
5. Fulton, J.; Hawkins, E.; Taylor, R.; Franzen, A. Yield monitor data: Collection, management, and usage. *Crops Soils* **2018**, *51*, 4–51. [CrossRef]
6. Ofori, E.; Griffin, T.; Yeager, E. Duration analyses of precision agriculture technology adoption: What's influencing farmers' time-to-adoption decisions? *Agric. Financ. Rev.* **2020**, *80*, 647–664. [CrossRef]
7. Schimmelpfennig, D. Farm Profits and Adoption of Precision Agriculture. USDA. *Econ. Res. Rep.* **2016**, *217*, 1–46. Available online: https://www.ers.usda.gov/webdocs/publications/80326/err-217.pdf?v=0 (accessed on 17 January 2023).
8. Lachia, N.; Pichon, L.; Marcq, P.; Taylor, J.; Tisseyre, B. Why are yield sensors seldom used by farmers–a French case study. In *Precision Agriculture '21*; Wageningen Academic Publishers: Budapest, Hungary, 2021; pp. 745–751. [CrossRef]
9. Pallottino, F.; Biocca, M.; Nardi, P.; Figorilli, S.; Menesatti, P.; Costa, C. Science mapping approach to analyze the research evolution on precision agriculture: World, EU and Italian situation. *Precis. Agric.* **2018**, *19*, 1011–1026. [CrossRef]
10. Weiss, M.; Jacob, F.; Duveiller, G. Remote sensing for agricultural applications: A meta-review. *Remote Sens. Environ.* **2020**, *236*, 111402. [CrossRef]
11. Maes, W.H.; Steppe, K. Perspectives for remote sensing with unmanned aerial vehicles in precision agriculture. *Trends Plant Sci.* **2019**, *24*, 152–164. [CrossRef]
12. Shirsath, P.B.; Sehgal, V.K.; Aggarwal, P.K. Downscaling regional crop yields to local scale using remote sensing. *Agriculture* **2020**, *10*, 58. [CrossRef]
13. Ali, A.M.; Abouelghar, M.A.; Belal, A.A.; Saleh, N.; Younes, M.; Selim, A.; Emam, M.E.; Elwesemy, A.; Kucher, D.E.; Magignan, S. Crop Yield Prediction Using Multi Sensors Remote Sensing. *Egypt. J. Remote Sens. Space Sci.* **2022**, *25*, 711–716.
14. Cantelaube, P.; Terres, J.-M. Seasonal weather forecasts for crop yield modelling in Europe. *Tellus A Dyn. Meteorol. Oceanogr.* **2005**, *57*, 476–487. [CrossRef]
15. Louhaichi, M.; Young, W.C.; Johnson, E.D. Reliability of Yield Mapping System for Estimating Perennial Ryegrass Seed Yield. *Aust. J. Basic Appl. Sci.* **2013**, *7*, 133–138.
16. Tsouros, D.C.; Bibi, S.; Sarigiannidis, P.G. A Review on UAV-Based Applications for Precision Agriculture. *Information* **2019**, *10*, 349. [CrossRef]
17. Wahab, I.; Hall, O.; Jirström, M. Remote Sensing of Yields: Application of UAV Imagery-Derived NDVI for Estimating Maize Vigor and Yields in Complex Farming Systems in Sub-Saharan Africa. *Drones* **2018**, *2*, 28. [CrossRef]
18. Wan, L.; Cen, H.; Zhu, J.; Zhang, J.; Zhu, Y.; Sun, D.; Du, X.; Zhai, L.; Weng, H.; Li, Y.; et al. Grain yield prediction of rice using multi-temporal UAV-based RGB and multispectral images and model transfer–a case study of small farmlands in the South of China. *Agrict. For. Meteorol.* **2020**, *291*, 108096. [CrossRef]
19. Rasmussen, J.; Ntakos, G.; Nielsen, J.; Svensgaard, J.; Poulsen, R.N.; Christensen, S. Are vegetation indices derived from consumer-grade cameras mounted on UAVs sufficiently reliable for assessing experimental plots? *Eur. J. Agron.* **2016**, *74*, 75–92. [CrossRef]
20. Jensen, S.M.; Akhter, M.J.; Azim, S.; Rasmussen, J. The predictive power of regression models to determine grass weed infestations in cereals based on drone imagery–statistical and practical aspects. *Agron.* **2021**, *11*, 2277. [CrossRef]
21. Bitarafan, Z.; Rasmussen, J.; Westergaard, J.C.; Andreasen, C. Seed yield and lodging assessment in red fescue (*Festuca rubra* L.) sprayed with trinexapac-ethyl. *Agronomy* **2019**, *9*, 617. [CrossRef]
22. Woebbecke, D.M.; Meyer, G.E.; von Bargen, K.; Mortensen, D.A. Color indices for weed identification under various soil, residue, and lighting conditions. *Trans. Am. Soc. Agric. Eng.* **1995**, *38*, 259–269. [CrossRef]
23. Gitelson, A.A.; Kaufman, Y.J.; Stark, R.; Rundquist, D. Novel algorithms for remote estimation of vegetation fraction. *Remote Sens. Environ.* **2002**, *80*, 76–87. [CrossRef]
24. Say, S.M.; Keskin, K.; Sehri, M.; Sekerli, Y.E. Adoption of precision agriculture technologies in developed and developing countries. *Online J. Sci. Technol.* **2018**, *8*, 7–15. Available online: https://www.tojned.net/journals/tojsat/articles/v08i01/v08i01-02.pdf (accessed on 17 January 2023).
25. Nowak, B. Precision Agriculture: Where do We Stand? A Review of the Adoption of Precision Agriculture Technologies on Field Crops Farms in Developed Countries. *Agric. Res.* **2021**, *10*, 515–522. [CrossRef]
26. Maloku, D. Adoption of precision farming technologies: USA and EU situation. *Pract. Appl. Sci.* **2020**, *VIII*, 7–14. Available online: https://seaopenresearch.eu/Journals/articles/SPAS_22_1.pdf (accessed on 17 January 2023).

27. Muruganantham, P.; Wibowo, S.; Grandhi, S.; Samrat, N.H.; Islam, N. A Systematic Literature Review on Crop Yield Prediction with Deep Learning and Remote Sensing. *Remote Sens.* **2022**, *14*, 1990. [CrossRef]

28. Hussain, N.; Sarfraz, S.; Javed, S. A Systematic Review on Crop-Yield Prediction through Unmanned Aerial Vehicles. In Proceedings of the 2021 16th International Conference on Emerging Technologies (ICET), Islamabad, Pakistan, 22–23 December 2021; IEEE: Manhattan, NY, USA, 2021; pp. 1–9.

29. Rasmussen, J.; Nielsen, J.; Streibig, J.C.; Jensen, J.E.; Pedersen, K.S.; Olsen, S.I. Pre-harvest weed mapping of *Cirsium arvense* in wheat and barley with off-the-shelf UAVs. *Precis. Agric.* **2019**, *20*, 983–999. Available online: https://link.springer.com/article/10.1007/s11119-018-09625-7 (accessed on 17 January 2023). [CrossRef]